Energy xxx (2014) 1–15

Contents lists available at ScienceDirect

Energy

journal homepage: www.elsevier.com/locate/energy

Single-fuel steam gasification of switchgrass and coal in a bubbling fluidized bed: A comprehensive parametric reference for co-gasification study

Mohammad S. Masnadi [a, *], John R. Grace [a], Xiaotao T. Bi [a], C.Jim Lim [a], Naoko Ellis [a], Yong Hua Li [b], A.Paul Watkinson [a, b]

[a] Clean Energy Research Centre, Department of Chemical and Biological Engineering, University of British Columbia, 2360 East Mall, Vancouver, BC V6T 1Z3, Canada
[b] Highbury Energy Inc., Suite 1820 Cathedral Place, 925 West Georgia Street, Vancouver, BC V6C 3L2, Canada

ARTICLE INFO

Article history:
Received 28 August 2014
Received in revised form
9 November 2014
Accepted 15 November 2014
Available online xxx

Keywords:
Steam gasification
Biomass
Coal
Alkali metals
Enhanced equilibrium modeling
Renewable energy

ABSTRACT

Recent regulatory sharp curbs on coal power plants have compelled industries to adopt alternative sources of fuels. Biomass/fossil fuel co-gasification could be a pathway through more sustainable energy production technologies. As a basis for co-gasification study, the characteristics of single-fuel switchgrass and coal steam gasification in an atmospheric pilot scale bubbling fluidized bed reactor were studied. Increasing the steam-to-fuel ratio at 860 °C caused a moderate increase in the H_2 and CO_2 concentrations and decreases in the CO and CH_4 concentrations, due to more steam-CH_4 reforming and water–gasification reaction of CO. With increasing reactor temperature, the H_2 concentration increased, whereas the CO, CH_4, and CO_2 concentrations fell slightly. Fall switchgrass gasification resulted in higher carbon, hydrogen and cold gas efficiencies than spring harvest gasification, possibly due to higher potassium concentration and hence, greater reactivity of the fall switchgrass. The equilibrium model was unable to predict the syngas composition properly. Adding an extra methanator stoichiometric reactor to produce methane based on the empirical CH_4 concentration, and removing part of the carbon, hydrogen and steam before introducing the feed and gas agent streams to the reactor based on experimental carbon, hydrogen, and steam efficiencies, the kinetically modified model predicted the syngas composition accurately.

1. Introduction

The combined average temperature over global land and ocean surfaces for January 2014 was the warmest since 2007 and the fourth warmest on record, 0.65 °C above the 20th century average [1]. The increasing GHG (greenhouse gas) concentrations and concern over the effect on climate [2–4] encourage indeed demand the development of new advanced energy cycles. Canada's total GHG (greenhouse gas) emissions in 2011 were 702 Mt (megatonnes) of carbon dioxide equivalent (CO_2 eq.), 19% (111 Mt) above the 1990 emissions of 591 Mt [5].

As part of a solution, renewable energy technologies currently supply ~18.5% of the world's primary energy supply, with bioenergy the largest contributor. In 2011, total biofuels supply was ~1311 Mtoe, accounting for 10% of the world's total primary energy supply and ~54% of its renewable energy supply [6]. Among bioenergy technologies, thermochemical conversion of solid fuels via gasification into synthesis gas (syngas) is a promising and diversified option. A main advantage compared to combustion is its downstream products diversity [7]. Although energy utilization from renewable sources will grow, fossil fuels are expected to remain the main source of energy and emissions for decades. Coal power plants are still contributing to about 42% of net electricity generation in the Unites States, and are projected to keep their lead until 2040 [8,9].

Panicum virgatum, commonly known as switchgrass, is a perennial warm-season bunchgrass native to North America.

* Corresponding author. Chemical & Biological Engineering Building, 2360 East Mall, Vancouver, BC V6T 1Z3, Canada. Tel.: +1 604 822 3121.
E-mail address: s.masnadi@gmail.com (M.S. Masnadi).

http://dx.doi.org/10.1016/j.energy.2014.11.054
0360-5442/

Switchgrass has potential as an energy crop for Eastern Canada [14] and for the US, where it was selected as a model herbaceous crop for the Oak Ridge National Laboratory's Biofuel Feedstock Development Program [15,16]. It shows promise due to its high productivity, appropriateness for marginal land quality, low water and nutritional requirements, environmental benefits, and flexibility for multipurpose uses [10]. Switchgrass ash is rich in AAEM (alkali and alkaline earth metals) and has potential to catalyze and enhance carbon gasification reactions [13,17,18,69]. A published review article [11] on the conversion of switchgrass to value-added products revealed that study of large scale gasification of switchgrass is rare.

In this paper therefore, switchgrass and coal were gasified separately in an atmospheric pilot-scale BFB (bubbling fluidized bed) reactor with pure steam as the agent to investigate the effects of different critical parameters on gasification performance. On the basis of this paper, the switchgrass/coal co-gasification study is developed and presented elsewhere [13]. To test the reliability of equilibrium modeling, a computer simulation was also presented and the product gas composition was predicted. This work provides reference data for a comprehensive study on co-gasification of biomass and fossil fuels with and without integrated CO_2 capture [12,13,17,18,68].

2. Materials and methods

2.1. Fuel characterization

Spring and fall harvest switchgrass from Ontario, Canada (Nott farm) and thermal coal from Vancouver Island, Canada (Quinsam mine) were tested in this study. The ASTM D346 and D346M-11 standard method were followed for feedstock sampling.

Table 1 presents the ultimate, proximate and elemental ash analyses of the parent fuels. As expected, the coal contained much higher carbon (80.3 wt%) and therefore heating value (28.4 MJ/kg) than the biomass. Fuel minerals act as in-situ catalysts to augment carbon thermochemical conversion [19]. Switchgrass ash is rich in potassium, 10.8 wt% for spring harvest switchgrass (SP-SG) and 21.8 wt% for fall harvest switchgrass (F-SG). The fall harvest variety was therefore expected to have higher reactivity, as it contained the highest potassium in its ash. More details on the morphology, surface area and thermogravimetric analyses of switchgrass can be found elsewhere [17,18,20]. The Quinsam mine coal is a thermal coal, with low crucible swelling index (0.5), suitable for fluidization applications. The amounts of undetermined species of the ash analyses were less than 3 wt% for all samples. Therefore, the "undetermined" in Table 1 is predominantly oxygen.

Table 1
Ultimate, proximate and ash analysis of fresh feedstocks for pilot-scale experiments.

Sample	Quinsam mine coal (Vancouver Island)	Spring switchgrass (Ontario) (SP-SG)	Fall switchgrass (Ontario) (F-SG)
Ultimate analysis (wt%), daf[a]			
Carbon, C	80.3	49.7	47.7
Hydrogen, H	5.5	6.2	5.9
Nitrogen, N	0.9	0.9	1.0
Sulfur, S	0.7	0.1	0.1
Oxygen, O (diff[b])	12.6	43.1	45.3
Proximate analysis (wt%)			
Moisture	4.25	9.26	11.63
Ash (db[a])	12.90	3.07	3.80
Volatile (db)	38.01	79.50	79.47
Fixed Carbon (db)	49.09	17.43	16.73
Higher heating value (db) (MJ/kg)	28.40	19.38	19.23
Crucible Swelling Number	0.5	n.a.	n.a.
Ash analysis (wt%)			
Si	16.87	20.14	14.60
Al	13.39	0.22	0.06
Ti	1.43	0.02	0.01
Fe	4.69	0.38	0.19
Ca	13.36	9.40	7.28
Mg	0.24	3.26	2.80
Na	0.16	0.09	0.02
K	0.06	**10.76**	**21.83**
P	0.24	2.2	3.13
S	2.30	2.15	1.35
Ba	0.01	0.02	0.01
Sr	0.07	0.01	0.01
Mn	0.05	0.05	0.03
Cr	0.00	0.01	0.01
Cu	0.03	0.01	0.01
Ni	0.02	0.00	0.01
V	0.05	0.01	0.00
Zn	0.01	0.02	0.03
Hg	0.00	0.04	0.02
Undetermined[c]	46.96	51.21	48.6

Both spring and fall switchgrass were rich in potassium (bold numbers).
[a] daf = dry and ash free, db = dry basis;
[b] Calculated by difference;
[c] Predominantly oxygen, since the inorganic elements are present as oxides (e.g., Al_2O_3, SiO_2, K_2O).

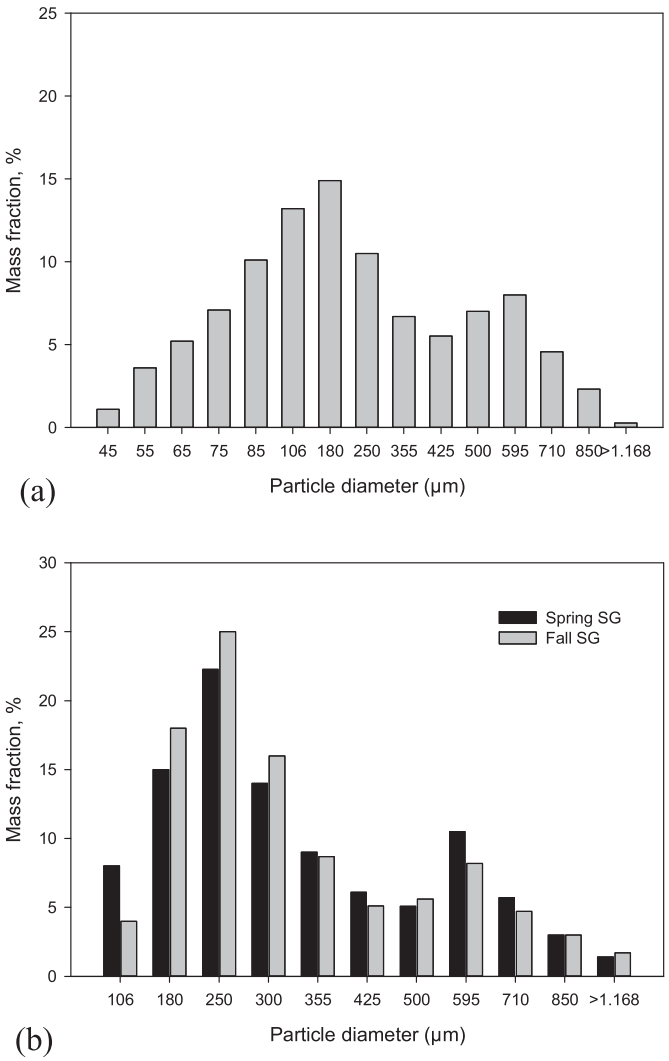

Fig. 1. Particle size distributions of (a) coal (b) spring and fall switchgrasses.

Please cite this article in press as: Masnadi MS, et al., Single-fuel steam gasification of switchgrass and coal in a bubbling fluidized bed: A comprehensive parametric reference for co-gasification study, Energy (2014), http://dx.doi.org/10.1016/j.energy.2014.11.054

All samples were crushed before the characterization analyses and gasification experiments. A C.S. Bell Co. hammer-mill with 1/16 inch (1.59 mm) screen openings and a FRITSCH disc-mill were used for biomass and fossil fuel crushing respectively. Both biomass and coal had bimodal particle size distributions, as shown in Fig. 1 (using standard sieves). The coal, SP-SG and F-SG bulk densities were 740, 235 and 242 kg/m^3, respectively.

2.2. Experimental apparatus and operation

Fluidized bed reactors are among the most promising types of gasifier, with excellent fuel mixing, carbon conversion and thermal efficiency. They are able to operate with flexible feed specification and size, and are potentially suitable for scale-up. Gasification of single (this paper) and mixture fuels [13] was studied in a pilot-scale fluidized bed reactor, with steam as the gasifying agent. Air gasification produces a gas with a low heating value (4–6 MJ/m^3) [21]. Steam helps to produce high-quality product gas with good heating value, rich in hydrogen.

Steam gasification was performed in the HEI (Highbury Energy Inc.) pilot-scale BFB (bubbling fluidized bed) reactor. This unit includes a high-temperature reactor tube inside a 305 mm ID high-pressure reactor shell, a screw feeder, steam super-heaters, a double cyclone, gas coolers, and a baghouse filter, as shown in Fig. 2. Fuel stored in the biomass storage hopper under N_2 was fed to the screw feeder's hopper through a 51 mm ball valve. The biomass in the feed hopper (Vibra Screw Inc.) was fed to the fluidized bed gasifier through a pneumatic conveyor through an 8.48 mm pipe, with N_2 as the conveying gas. A Vibra Screw Inc. electric vibrator attached to the feeder hopper helped propel fuels into the pipe.

The gasifier consisted of a 102 mm ID, 1219 mm long, stainless steel (800H/HT, S40, SMLS) pipe as an inner reactor with a gas distributor installed above the steam entrance, as shown in Fig. 3. An internal cyclone (63 mm ID) was installed at the top of the column, immediately upstream of where the producer gases exit, to separate entrained solids from the gas stream, and to reduce the tar content of the gases. Pfeifer et al. [22] showed that the hot surface of an internal cyclone can thermally crack tars. The reactor is heated by two semi-cylindrical (127 mm ID, 229 mm OD, 914 mm L) ceramic fiber electrical heaters (240 V 4200 W each) and one full cylindrical (127 mm ID, 152 mm L) ceramic fiber electrical heater (120 V 1400 W) on the top section. Saturated steam from the laboratory steam line (586 kPa$_g$, 160 °C) is supplied to the gasifier through a steam flow meter to the steam super-heaters (12 × 240 V × 1800 W), super-heated to about 800 °C, before entering the gasifier. N_2 is introduced for purging and preheating. The product syngas leaves the gasifier through double external cyclones to water-cooled double-pipe heat exchanger gas coolers. The cooled syngas passes through an orifice plate before entering a baghouse filter, and then continuing to a rooftop burner. A compressed air supply system was installed for optional biomass combustion preheating or biomass air-steam gasification [23].

Silica sand (Lane Mountain Company, Washington) was chosen as the inert fluidization bed material for the process. The sand improves the agitation in the fluidized bed, while also providing high rates of heat and mass transfer. It also decreases the tendency of fuel particles to agglomerate at the operating conditions [24]. Olivine sand, dolomite, and lime can also be used. However attrition of dolomite and lime is significant. The sand was sieved to 300–355 μm (US mesh #45–50) (resulting in Geldart group B particles). The static bed height for all experiments was ~0.30 m. This height was thought to be optimal for temperature distribution in the column based on previous HEI experiments [23]. The sand composition is shown in Table 2. Key particle properties are listed in Table 3, with super-heated steam (at 525 °C and 1 atm) as fluid and the bubbling bed operated at an inlet superficial gas velocity of ~0.37 m/s.

The product gas composition was measured by Varian Inc. CP-4900 on-line micro GC (gas chromatograph) every 4 min during operation, with a Molsieve column for H_2, CO, N_2, and CH_4 detection. Carbon dioxide was measured using a CP-PoraPLOT U column. The GC was calibrated using Praxair standard gas before the experiments. Product gas moisture and tar were fully removed by a shell and tube condenser, a silica-gel column, and a Genie membrane separator before being introduced to the GC. Helium was the

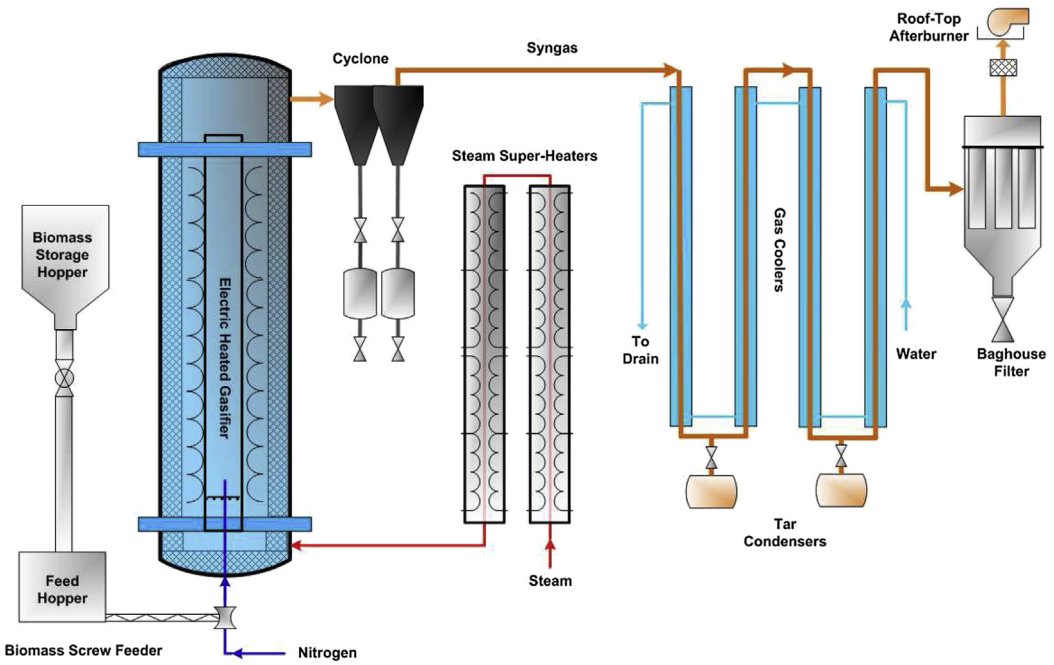

Fig. 2. Schematic of Highbury Energy Inc. (HEI) pilot-scale bubbling fluidized bed reactor (adapted from HEI).

Please cite this article in press as: Masnadi MS, et al., Single-fuel steam gasification of switchgrass and coal in a bubbling fluidized bed: A comprehensive parametric reference for co-gasification study, Energy (2014), http://dx.doi.org/10.1016/j.energy.2014.11.054

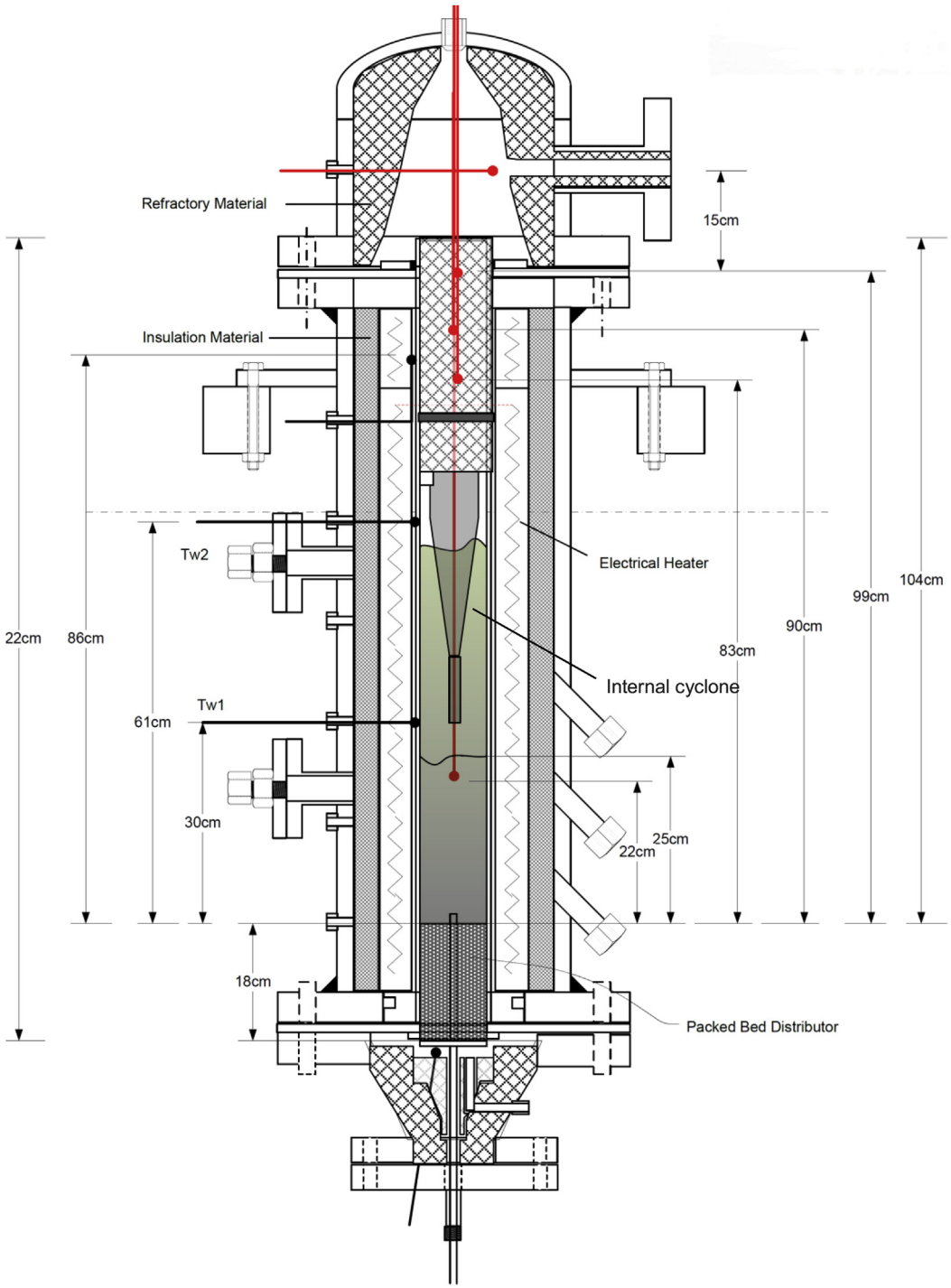

Fig. 3. Detailed dimensions of bubbling fluidized bed gasifier (not to scale) (drawing provided by HEI).

GC carrier gas. The gas measurement port was downstream of the heat exchangers and before the baghouse filter (see Fig. 2). The reported gas compositions are all on a N_2-free basis, i.e. excluding the nitrogen which conveys the feed into the reactor.

Table 2
Silica sand analysis.

CaO	MgO	Al_2O_3	Fe_2O_3	K_2O	Na_2O	SiO_2
0.04	0.02	0.64	0.15	0.27	0.08	98.14

A modified version of European protocol CEN/TS 15439 [27] was used for tar sampling of the product gas. The tar sampling port was branched from the main exit pipe located at the top of the gasifier. The port was heated by a rope-heater and insulated to keep the stream temperature above 300 °C, thereby preventing tar condensation along the pipe. A XC-60 Apex source sampling console which includes a gas meter, sample pump and temperature control probe sampled the product syngas during operation. The product gas first passed through a glass fiber filter to remove fine particles. Next, the filtered gas entered six impinger bottles in

Please cite this article in press as: Masnadi MS, et al., Single-fuel steam gasification of switchgrass and coal in a bubbling fluidized bed: A comprehensive parametric reference for co-gasification study, Energy (2014), http://dx.doi.org/10.1016/j.energy.2014.11.054

Table 3
Material and hydrodynamic properties (based on steam at 525 °C and 1 atm).

Material	ρ_b (kg/m^3) (bulk)	d_s (μm)	U_t (m/s)[b]	U_{mf} (m/s)[c]
Silica sand	1600	327.5	1.24	0.064
Coal	740	142[a]	0.44	0.007
SP-SG	235	264[a]	0.45	0.008
F-SG	242	274[a]	0.47	0.009

[a] Based on $d_s = 1/\sum_i(\frac{x_i}{d_{si}})$;
[b] Calculated based on Haider and Levenspiel [25] correlation;
[c] Calculated based on Grace [26] equation.

series, each containing 50 ml of iso-propanol solvent. All six impingers were kept at −20 °C in a salt ice bath. After tar sampling, the bottles were rinsed with extra solvent to collect the entire tar from the bottles. Then, the captured tar/solvent mixture was re-filtered through a 0.02 μm filter to remove particles. The collected solvent/tar mixture was thermally treated in a rotary evaporator at 55 °C and 17 kPa until the solvent was fully extracted, taken once the drip rate in the evaporator had fallen to one every 4 s. To remove the remaining water from the tar, 50 ml ethanol was added and thermal treatment was continued. Evaporation continued until a drip rate of one every 4 s was reached. Air flow into the vacuum flask was then initiated, with the vacuum held below 68 kPa. This procedure removed the remaining water droplets [27]. Air flow continued for 20 min. The vacuum flask was then removed, allowing it to be cooled in a desiccator and weighed to determine the quality of the product.

As shown in Fig. 2, the unreacted steam condensed downstream in a shell and tube heat exchanger. This water was then treated and reused as a gasification agent. The TOC (total organic carbon) content of the water sample of each run was analyzed in triplicate by a TOC analyzer (Shimadzu TOC-VCPH). The organic carbon was measured by the NPOC (non-purgeable organic carbon) method, based on purging volatile organic carbon of the acidified sample using inert gas (nitrogen). Inorganic carbon is converted to carbon dioxide through acidification, and the remaining carbon content is oxidized to carbon dioxide through high-temperature catalytic oxidation. The TSS (total suspended solids) [28] of the water samples were measured using a Whatman 934-AH filter.

To assess the process technology, the following variables were determined:

Carbon conversion efficiency, η_C

$$\eta_C = \frac{\overbrace{v_{gas}*1000*[CH_4\% + CO\% + CO_2\%]*12/22.4}^{Mass\ of\ C\ in\ the\ product\ gas}}{\underbrace{m_{fuel,dry}(1-x_{ash})*C\%}_{Mass\ of\ C\ in\ the\ fuel}} \quad (1)$$

Hydrogen conversion efficiency, η_H

$$\eta_H = \frac{\overbrace{v_{gas}*1000*[2H_2\% + 4CH_4]/22.4}^{Mass\ of\ H\ in\ the\ product\ gas}}{\underbrace{(m_{fuel,dry}(1-x_{ash})*H\%) + (2*m_{fuel,wet}*H_2O\%/18.0) + (2*m_{steam}/18.0)}_{Mass\ of\ H\ in\ the\ inlet}} \quad (2)$$

where CH_4%, CO%, CO_2% and H_2 (vol%) are gas concentrations, v_{gas} (Nm^3/h) is the dry gas flow rate, $m_{fuel,dry}$ and $m_{fuel,wet}$ are the dry and wet fuel feeding rates (g/h) respectively, x_{ash} is the ash content in the feed, C% and H% are the carbon and hydrogen contents (weight based) in the ultimate analysis of fuel, respectively, and m_{steam} (g/h) is the steam mass flow rate. The steam produced was not factored into the hydrogen utilization equation, as it was too difficult to measure in the current reactor setup.

The cold gas efficiency, η_{cg}

$$\eta_{cg} = \frac{m_{gas}*Q_{gas}}{m_{fuel,dry}*Q_{fuel}} \quad (3)$$

where m_{gas} (g/h) is the dry gas mas flow rate, and Q_{gas} (MJ/g) and Q_{fuel} (MJ/g) are the product gas and fuel heating values, respectively. In the present work, the cold gas efficiency is of limited significance, as it misses the heat from the electrical steam superheaters, and the walls of the reactors.

The dry gas (N_2-free) HHV (higher heating value) at the standard state of 101.3 kPa and 273 K can be estimated from the gas composition by

$$HHV = 12.7H_2\% + 12.6CO\% + 39.8CH_4\% + 70C_2H_6\% + 63C_2H_4\% + 92C_3H_6\% + 100C_3H_8\% + 123C_4H_8\% \quad (4)$$

where the species heats of combustion are in MJ/N m^3. This equation is based on heat of combustion data [29], assuming ideal-gas behavior for the gaseous species. The micro-GC was not able to measure the concentrations of higher hydrocarbons (e.g. ethylene), which are often too low to be detected. However, accurate measurements of them is crucial when the gasifier operates at temperatures below 700 °C or at elevated pressure, as the gas heating value can be significantly altered by the presence of even small fractions of these hydrocarbons.

The mass-based steam-to-fuel ratio, SF, is defined by

$$SF = \frac{m_{steam}}{m_{fuel,dry}} \quad (5)$$

In this work, the error bars are based on 95% confidence intervals for a population mean (assuming a normal distribution).

The significant gasification reactions in this work are:

(1) Pyrolysis:

$$Fuel + Heat \rightarrow Char,\ H_2,\ CO,\ CO_2,\ H_2O,\ CH_4,\ C_nH_m,\ Tars,\ \ldots \quad (6)$$

(2) Tar cracking:

$$Tar + Heat \rightarrow H_2 + CO + CO_2 + \ldots \quad (7)$$

(3) Combustion (oxidation):

$$C + 1/2O_2 \rightarrow CO + 110.6\ kJ/mol \quad (8)$$

$$C + O_2 \rightarrow CO_2 + 393.8\ kJ/mol \quad (9)$$

$$CO + 1/2O_2 \rightarrow CO_2 + 283.2\ kJ/mol \quad (10)$$

Please cite this article in press as: Masnadi MS, et al., Single-fuel steam gasification of switchgrass and coal in a bubbling fluidized bed: A comprehensive parametric reference for co-gasification study, Energy (2014), http://dx.doi.org/10.1016/j.energy.2014.11.054

(4) Boudouard reaction:

$$C + CO_2 \leftrightarrow 2CO \ - 172.6\ kJ/mol \quad (11)$$

(5) Steam-carbon reactions:

$$C + H_2O \leftrightarrow H_2 + CO \ - 131.2\ kJ/mol \quad (12)$$

$$C + 2H_2O \leftrightarrow 2H_2 + CO_2 \ - 89.8 kJ/mol \quad (13)$$

(6) Methanation:

$$C + 2H_2 \leftrightarrow CH_4 + 74.9\ kJ/mol \quad (14)$$

(7) CO shift (water-gas shift):

$$CO + H_2O \leftrightarrow CO_2 + H_2 + 41.4\ kJ/mol \quad (15)$$

(8) Steam-methane reforming:

$$CH_4 + H_2O \leftrightarrow CO + 3H_2 \ - \ 206.1\ kJ/mol \quad (16)$$

2.3. Simulation method

Equilibrium models can predict thermodynamic boundaries as a guide for process design, assessment and improvement. At chemical equilibrium, a reacting system is at its most stable composition, a condition achieved when the entropy of the system is maximized, while its Gibbs free energy is minimized. Two approaches are available for equilibrium modeling: stoichiometric and non-stoichiometric [53]. The stoichiometric approach requires a clearly defined reaction mechanism incorporating all chemical reactions and species involved. In non-stoichiometric formulations, on the other hand, no particular reaction mechanisms or species are involved in the numerical solution. The only input needed to specify the feed is the elemental composition, which can be readily obtained from the ultimate analysis. The later formulation is particularly suitable for systems with unclear reaction mechanisms and feed streams like biomass whose precise chemical compositions are unknown [54]. Both methods were applied in this project, and similar results were obtained. Reactions (8)–(16) were considered for the stoichiometric approach.

The "solid simulation class" of Aspen Plus V7.2 process simulator was used for the equilibrium simulation. The process flowsheet considered three stages: reaction, cooling, and separation. The Peng-Robinson model [55] was used as the thermodynamic equation of state for the simulation. First, the ultimate and proximate analyses of the fuel (switchgrass or coal) were specified. All species were defined as "conventional", except for C as solid and ash as a "NC (non-conventional)" component. The fuel stream then entered the decomposition (yield) reactor where the fuel was converted into its constituent components - carbon, hydrogen, oxygen, sulfur, nitrogen, and ash - by specifying the yield distribution according to the fuel ultimate analysis. The heat generated from the yield reactor was transferred to the endothermic gasifier (RGibbs). The feed and steam streams were then activated, the reactor temperature and pressure determined, and the system Gibbs free energy minimized to yield the products. The product stream was next cooled to 25 °C using a shell-tube heat exchanger, and ash/solid particles were separated using a solid splitter. More details are provided elsewhere [12]. Assumptions included steady state conditions, isothermal reactor, instantaneous drying and pyrolysis in the gasifier [56] and the components listed in Table 4 as the only species considered.

Table 4
Species included in the equilibrium simulation.

Class	Chemical formula
A	CH_4, C_2H_2, C_2H_4, C_2H_6, C_3H_8
B	H, H_2, O, O_2, CO, CO_2, H_2O, H_2O_2, HO_2
C	N_2, NH_3, N_2O, NO, NO_2, NO_3, HCN
D	S, SO, SO_2, SO_3, COS, CS, CS_2, H_2S
E	C (s), Ash

3. Results and discussions

3.1. Experimental study

3.1.1. 100% Quinsam mine coal gasification

To study the effect of biomass on coal gasification in a pilot-scale fluidized bed reactor, single feedstocks were first gasified. Fig. 4 shows typical dynamic results for a dry nitrogen-free product gas composition and bed temperature with different fuel feed rates. The bed thermocouple was at height ~0.2 m above the distributer. Time (t) 0 corresponds to the start of feeding fuel to the reactor. As steam gasification is an endothermic process, introducing coal to the reactor caused a sharp drop in bed temperature. The temperature and gas concentration were relatively stable during the experiment. The endothermic gasification reactions (e.g. methane reforming, (16) and steam-carbon reactions (12) and (13)) dominated, and the product gas was rich in hydrogen. It is evident from Fig. 4 that increasing the coal feed rate, caused the bed temperature to drop slightly, as more heat was required at lower steam-to-coal ratios. The produced gas H_2:CO ratio (~4:1) is suitable for methanol and ammonia synthesis [7].

Fig. 5 shows the effect of steam-to-coal mass ratio (SF) on gas composition for a limited range of temperatures. Even for the narrow range of steam-to-coal ratios covered during the gasification run, there was a visible effect of SF on the product gas composition. Increasing the steam-to-coal ratio caused a moderate increase in the H_2 and CO_2 concentrations and decreases in the CO and CH_4 concentrations. This can be explained by more steam reforming of CH_4 and more water-gas shift reaction of CO taking place because of the increased steam. The results are in good agreement with data in the literature [30–33].

Herguido et al. [31] reported that at temperatures above 750 °C, the water-gas shift reaction is in equilibrium at the exit of the gasifier freeboard. However in this work, comparison between the equilibrium constants of gasification reactions (8)–(16) and corresponding values obtained experimentally which should be equal if equilibrium has been reached, showed that the closest agreement was for the reaction (12), for which comparison is shown in Fig. 6. The discrepancy between our result and the Herguido et al. [31] conclusion is likely due to the location of our gas measurement port and GC, far beyond the reactor freeboard and condensers and before the baghouse filter (see Fig. 2) where the product gas temperature was below 50 °C. Maniatis and Buekens [44] also observed an important departure from the water-gas shift equilibrium in the exit gas at low temperatures. Note that the H_2O partial pressures for calculating the experimental data of Fig. 6 were indirectly estimated based on the H_2 molar balance.

Fig. 7 plots the carbon, hydrogen and cold gas efficiencies, as well as gas yield and product gas higher heating value vs. SF. It appears that higher feed rates (lower SF) resulted in higher HHV due to a higher CH_4 concentration (see Fig. 5). The carbon and cold gas efficiencies were less than 40% during the experiment, due to high fixed carbon and low coal reactivity. These efficiencies increased with increasing steam flow rate due to advancement of the steam-carbon, water-gas shift and steam-methane reforming reactions. The high fixed carbon of the solid particles captured by

Please cite this article in press as: Masnadi MS, et al., Single-fuel steam gasification of switchgrass and coal in a bubbling fluidized bed: A comprehensive parametric reference for co-gasification study, Energy (2014), http://dx.doi.org/10.1016/j.energy.2014.11.054

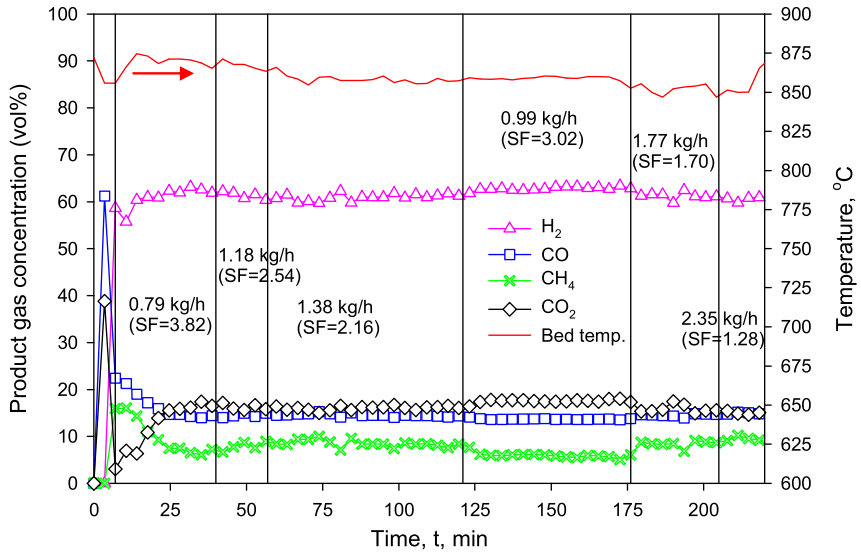

Fig. 4. Gasification results for dry nitrogen-free product gas composition and local bed temperature for 100% coal run with different coal dry basis (db) feed rates at atmospheric pressure. The bed thermocouple was ~0.2 m above the distributor.

the external cyclones confirms this, as shown in Table 5. The unreacted coal particles and chars caused pressure build-up and gradual blockage downstream. Recirculating entrained material to the bed can enhance the gasifier efficiency. The hydrogen efficiency increased slightly with increasing fuel feed rate, presumably due to higher methane production at lower SF.

3.1.2. 100% spring switchgrass (SP-SG) gasification

The gasification of biomass differed greatly from the gasification of coal. Biomass fuels tend to have considerably more volatile matter than coal. Hence, char gasification plays a minor role in the gasification of biomass because char typically represents less than 30 wt% of the pyrolysis products. Thus, devolatilization and secondary reactions play critical roles in determining the product distribution during biomass gasification [34,35].

The reactor reached steady-state after ~60 min Fig. 8 shows the effect of the steam-to-biomass mass ratio (SF) on the product gas composition. The temperature corresponding to each concentration data point is also presented. As for the 100% coal run, increasing the SF increased the H_2 yield and decreased the CH_4 product gas concentration. The largest error bars are for SF = 3.58, corresponding to the early stages of gasification when the compositions had not yet reached steady-state. Supplying extra steam as a gasifying agent increased the partial pressure of H_2O inside the gasification chamber, favoring the steam-carbon, water-gas shift and methane reforming reactions (reactions (12), (15) and (16)), leading to increased H_2 production [36]. However, the gasification temperature needs to be high enough (above 750–800 °C) for the steam reforming and water gas reactions to be favorable [37–39]. The CO/H_2 molar ratio for the SP-SG run was greater than for 100% coal due to biomass having higher volatile and oxygen contents (see Table 1). Based on Le Chatelier's principle, higher oxygen helps the oxidation and partial oxidation reactions. The CO_2 produced from the oxidation reactions can then react via the Boudouard reaction, reaction (11), producing CO. As noted above, potassium can catalyze the Boudouard and steam-carbon reactions. From Fig. 8 it can be seen that biomass steam gasification produces less CO_2 than coal gasification (cf. Fig. 5).

Yang et al. [45] reported that cellulose (rich in biomass) contributes mostly to the release of CO and volatiles, whereas

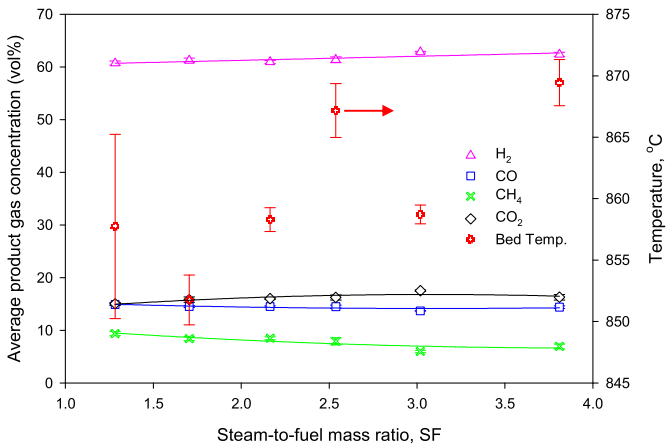

Fig. 5. Effect of steam-to-fuel (coal) ratio on gas composition at different temperatures at atmospheric pressure and a narrow range of temperature. The bed thermocouple was ~0.2 m above the distributor.

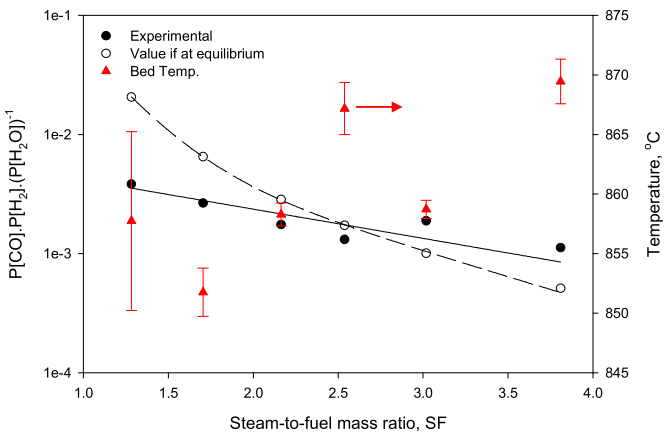

Fig. 6. Comparison between the equilibrium constant and concentration product that should be equal if thermodynamic equilibrium has been reached for steam-carbon reaction (12) for different SF at temperatures of 852–870 °C.

Please cite this article in press as: Masnadi MS, et al., Single-fuel steam gasification of switchgrass and coal in a bubbling fluidized bed: A comprehensive parametric reference for co-gasification study, Energy (2014), http://dx.doi.org/10.1016/j.energy.2014.11.054

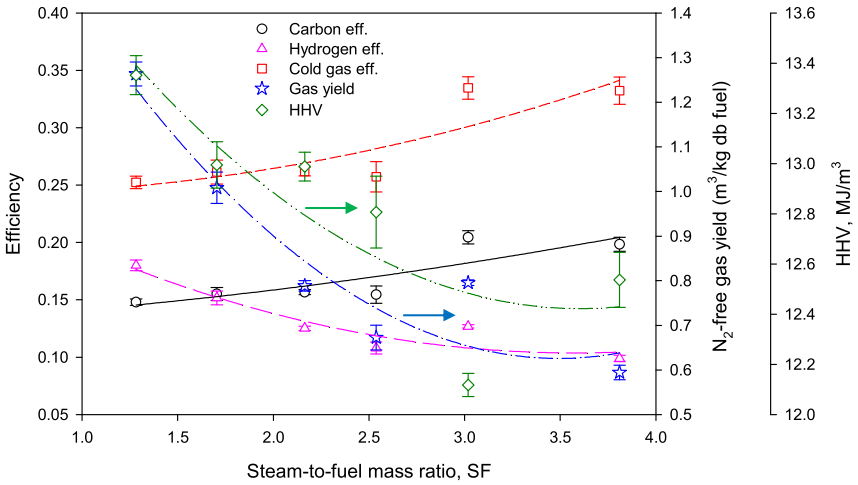

Fig. 7. Coal gasification carbon efficiency, hydrogen efficiency, cold gas efficiency, gas yield, and product gas higher heating value vs. SF in atmospheric pressure gasification.

hemicelluloses contributes mostly to CO_2, and lignin (rich in coal) to H_2,CH_4 and char. Their explanation is that for lignin decomposition, H_2 is released during cracking and deformation of aromatic C═C and C–H bonds, while CH_4 is released during cracking of methoxyl groups; for cellulose which is high in carbonyl groups, CO is released and for hemicelluloses rich in carboxyl, CO_2 is released [11].

Fig. 9 shows that biomass gasification led to much higher carbon and cold gas efficiencies than coal gasification (see the Supplementary material for data comparison). This is due to biomass being much more reactive than coal [17,18,20]. Potassium also enhanced the reactivity of the biomass (see Table 1). Fewer particles were separated and captured by the external cyclone for biomass than for the coal, indicating that most of the fuel was converted to gaseous products. The proximate analysis of the captured solids is provided in Table 6. No blockage or pressure build-up was observed during the biomass gasification experiment. The higher heating value of product gas did not change significantly (Fig. 9), as the gas composition followed a very similar trend for different biomass feed rates. It is evident from Fig. 9 that for SF increasing from 1.87 to 3.58, the gas yield, HHV, carbon conversion efficiency, and cold gas efficiency all decreased, which can be explained by the excessive quantity of low-temperature steam, lowering the reaction temperature, thereby decreasing the reaction rates and degrading the gas quality [30].

3.1.3. 100% fall switchgrass (F-SG) gasification

The fall switchgrass steam gasification experiment was performed at ~862 °C and atmospheric pressure, with a steam-to-biomass ratio of SF = 2.4. The effect of bed temperature on the gas product composition and HHV for F-SG steam gasification at almost constant steam-to-biomass ratio (SF ≈ 2.4) is presented in Fig. 10. The H_2 concentration clearly increased with increasing temperature, whereas the CH_4 concentration decreased. From Le Chatelier's principle, higher temperatures favor reactants in exothermic reactions and products in endothermic reactions. Therefore, endothermic reactions (e.g. steam-methane reforming, steam-carbon reaction) were more important at higher temperature, resulting in increased H_2 concentration and a drop in CH_4 concentration. Hence raising the temperature improved the hydrogen yield. At temperatures above 670 °C, the water-gas shift reaction dominated the process, resulting in decreased CO and increased H_2 concentrations. The contents of CO and CO_2 also depend on combustion reactions which are exothermic [30]. Thus, higher temperature was not favorable for CO and CO_2 production. At temperatures close to 900 °C, steam reforming and the Boudouard reactions dominate, resulting in CO production and CO_2 consumption [36]. The concentrations of higher hydrocarbons could not be measured in our experiments. It is likely that they show a downward trend with increasing temperature due to thermal cracking and steam reforming [30,32]. Increasing temperature slightly reduced the HHV of the product gas from 14.84 MJ/m^3 at ~700 °C to 14.50 MJ/m^3 at ~860 °C, due to decreases in CH_4 and CO concentrations. Fig. 10 also shows that the H_2 concentration increased and the CO concentration decreased relative to the corresponding results in Fig. 8. This might be due to different ash compositions of spring and fall switchgrass samples, affecting the degree of catalysis.

Table 5
100% coal proximate analysis of entrained particles captured by external cyclones.

	Moisture	Ash and sand (db[a])	Volatiles (db)	Fixed carbon (db)
Proximate analysis	8.6	46.7	4.7	48.6

[a] Dry basis.

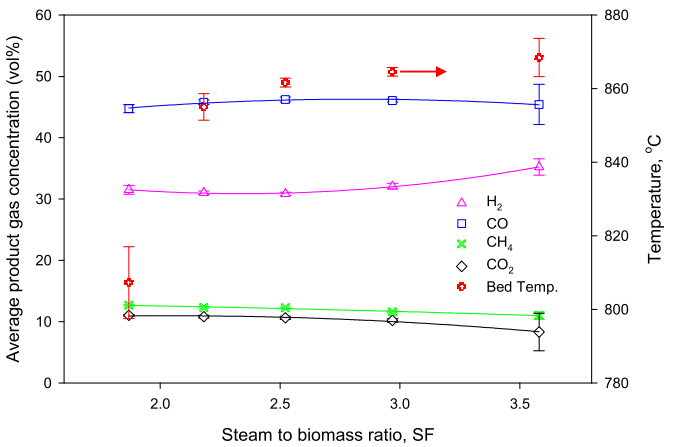

Fig. 8. Effect of steam-to-fuel (biomass) ratio on steady-state dry nitrogen-free gas composition at different temperatures and atmospheric pressure. The bed thermocouple was ~0.2 m above the distributer.

Please cite this article in press as: Masnadi MS, et al., Single-fuel steam gasification of switchgrass and coal in a bubbling fluidized bed: A comprehensive parametric reference for co-gasification study, Energy (2014), http://dx.doi.org/10.1016/j.energy.2014.11.054

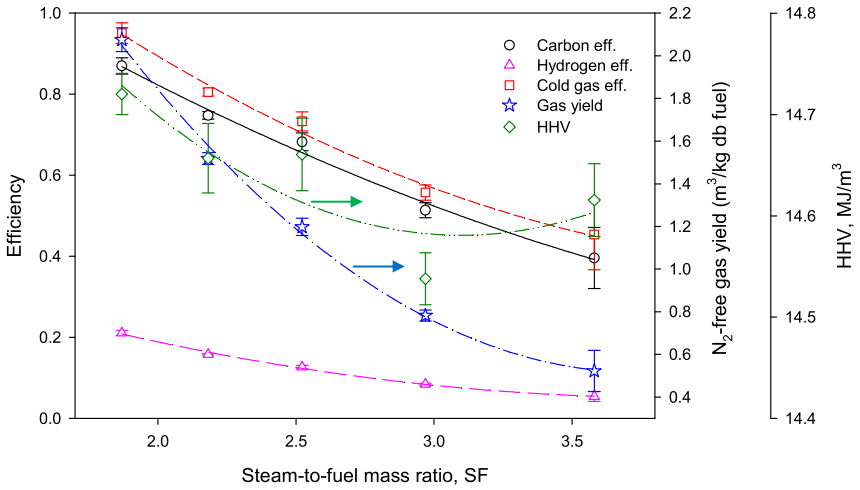

Fig. 9. SP-SG gasification carbon efficiency, hydrogen efficiency, cold gas efficiency, gas yield, and product gas higher heating value vs. SF in atmospheric pressure gasification.

Gupta and Cichonski [38] observed significant increases in H_2 concentration above 800 °C for SF between 0.5 and 1.08. The maximum H_2 yield was obtained at 1000 °C for a feedstock consisting of paper, and at 900 °C for cardboard and wood pellet feedstocks. González et al. [40] observed that in air gasification, the H_2 and CO concentrations increased from 700 to 900 °C, whereas those of CH_4 and CO_2 decreased. Turn et al. [32] found that for a temperature increase from 750 to 950 °C, the H_2 concentration increased from 31 to 45%, while the CH_4 and CO concentrations remained nearly constant, CO_2 decreased and the gas yield increased.

All gasification reaction (8)–(16) equilibrium constants and corresponding experimental values that should be equal if equilibrium has been reached were calculated and compared at different reactor bed temperatures. It was again found that steam-carbon reaction (13) had the best match. As shown in Fig. 11, the experimental estimates were below the equilibrium values at low temperatures because of relatively low hydrogen and carbon efficiencies. However, Fig. 11 shows how the experimental values of the gas composition approach the equilibrium values above 780 °C due to a progressive increase of the H_2 and a decrease of H_2O concentrations. This is consistent with Fig. 10 and higher fuel/steam conversion at higher temperatures, as discussed below.

The effects of temperature on hydrogen efficiency, carbon efficiency, cold gas efficiency, and gas yield of fall switchgrass gasification for SF ≈ 2.4 are shown in Fig. 12. All gasification performance parameters increased with increasing temperature for the range covered. Higher temperature resulted in increased gas yield because of higher conversion efficiencies. F-SG gasification resulted in higher carbon, hydrogen and cold gas efficiencies than SP-SG gasification, likely due to the higher potassium concentration of the F-SG. The N_2-free gas yield also increased from 0.98 m^3/kg for SP-SG to 1.10 m^3/kg biomass (db) for F-SG (see the Supplementary material for data comparison). Additional supporting data on the effect of biomass minerals on gasification performance are provided elsewhere [13,17,18,69].

Table 6
Proximate analysis of particles captured by external cyclones 1 and 2 for 100% SP-SG.

	Moisture	Ash and sand (db)	Volatile (db)	Fixed carbon (db)
Proximate analysis	5.3	62.4	5.6	32

It has been observed [41,42] that higher temperatures (700–950 °C) increase the gas yield and overall energy content of the gas. Kumar [36] reported that an increase in temperature (furnace set point from 750 to 850 °C) led to increases in energy and carbon conversion efficiencies and percent gas compositions of H_2. Boateng et al. [43] reported that an increase in gasification temperature from 700 to 800 °C caused increases in the gas yield, energy efficiency, carbon conversion efficiency and H_2 content, whereas the CH_4, CO and CO_2 contents all decreased. The decrease in CO content may have been due to the relatively low temperatures needed for the Boudouard reaction to predominate [36]. Lv et al. [30] also observed that the gas yield and carbon conversion efficiency generally increased with increasing temperature.

3.1.4. Tar and water sampling results

Fig. 13 presents the product gas tar yield (with and without N_2) for different steam gasification runs, based on the tar sampling standard method explained in section 2. The average bed temperature of different runs during the tar sampling period is indicated by the secondary *Y* axis. As the bed temperature for all runs is above 800 °C, the tars are likely PAH (polycyclic aromatic hydrocarbons) [46]. Typically, gasification of biomass results in higher tar yield with greater amount of stable aromatics than for coal gasification

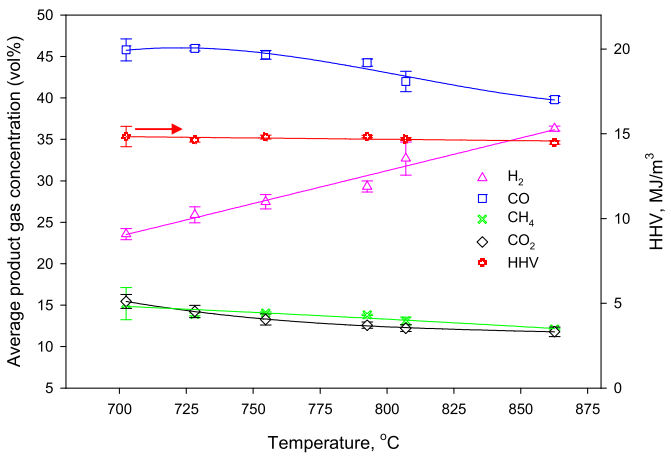

Fig. 10. Effect of temperature on dry nitrogen-free gas composition of 100% F-SG gasification for SF ≈ 2.4 at atmospheric pressure. The bed thermocouple was ~0.2 m above the distributor.

Please cite this article in press as: Masnadi MS, et al., Single-fuel steam gasification of switchgrass and coal in a bubbling fluidized bed: A comprehensive parametric reference for co-gasification study, Energy (2014), http://dx.doi.org/10.1016/j.energy.2014.11.054

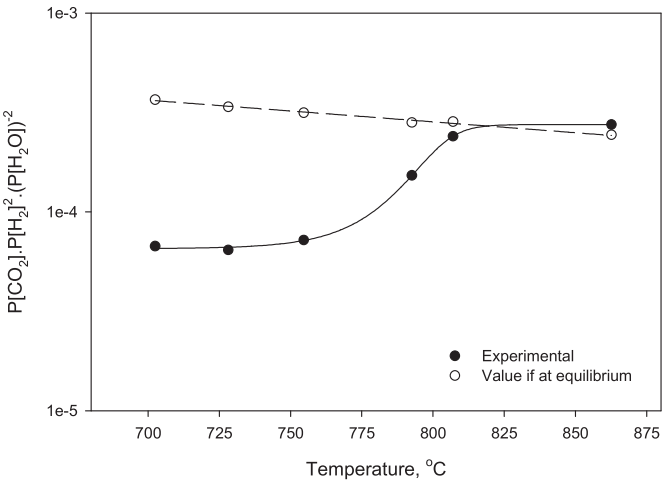

Fig. 11. Effect of gasification bed temperature on the 100% F-SG equilibrium constant and concentrations product that should be the same if equilibrium has been reached of the steam-carbon reaction for SF ≈ 2.4. The bed thermocouple was ~0.2 m above the distributor.

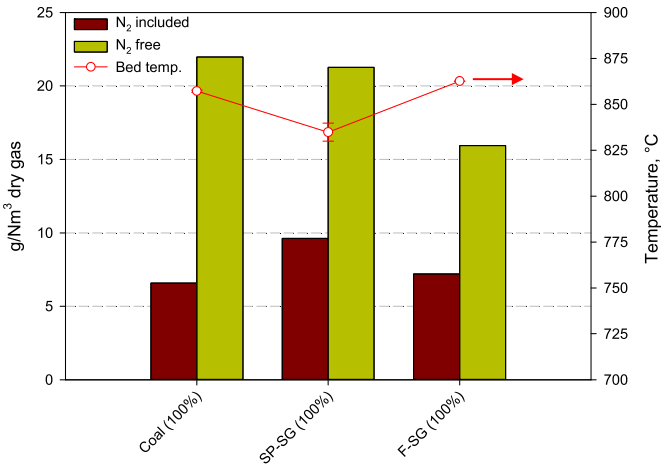

Fig. 13. Product gas tar yield (N_2 included and N_2-free) and bed temperature for steam gasification of 100% coal, 100% SP-SG and 100% in a bubbling fluidized bed (atmospheric pressure). The bed thermocouple was ~0.2 m above the distributor.

[47]. However, this seems not to be the case in Fig. 13, as the Vancouver Island coal is classified as "high volatile coal". F-SG gasification resulted in lower tar yield due to higher average bed temperature causing thermal tar cracking and higher ash and alkali metal contents than for SP-SG gasification. Many previous authors have found that alkali metal catalysts are effective in reforming tars [48–52]. The allowable tar content for IC (internal combustion) engines for power generation is <100 mg/Nm^3 [46]. Therefore, extra thermal or chemical tar cracking treatments are required to enhance the quality of the product gas before feeding it to an engine.

Condensed water samples from the steam gasification runs were analyzed by the standard measurement procedures briefly explained in Section 2 to determine the total organic carbon and total suspended solids. Results are shown in Fig. 14. As the gas yields of the 100% biomass gasification runs were higher than for the 100% coal, the TOCs for the pure biomass experiments were greater than for the coal steam gasification. Tars containing heterocyclic aromatics with high polarity are soluble in water (e.g. pyridine, phenols and cresols) [46].

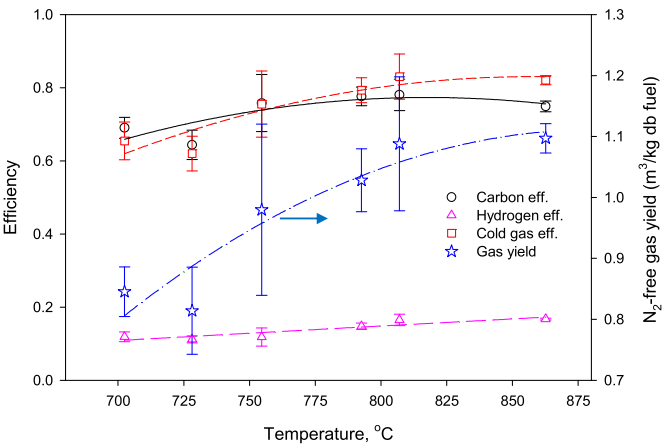

Fig. 12. Effect of bed temperature on hydrogen efficiency, carbon efficiency, cold gas efficiency, and gas yield for 100% F-SG gasification with SF ≈ 2.4 at atmospheric pressure. The bed thermocouple was ~0.2 m above the distributor.

3.2. Modeling

3.2.1. Equilibrium modeling results

There is a considerable advantage to gasifying under pressure, with the result that practically all modern processes operate at pressures of at least 10 bar, some as high as 100 bar [57]. Fig. 15 shows the effect of temperature and pressure on the H_2, CO, CH_4 and CO_2 equilibrium concentrations and HHV contours for the 100% F-SG steam gasification with SF = 2.41. The endothermic methane reforming, water gasification, and Boudouard reactions are enhanced by increasing the reactor temperature, resulting in an increase in H_2 and CO concentrations, whereas at lower temperatures, forward oxidation and methanation reactions are more active, causing an increase in CH_4 and CO_2 concentrations. An increase in pressure produces increased CH_4 and CO_2 concentrations, to the detriment of H_2 and CO, as, in accordance with Le *Chatelier's principle, an* increase in pressure shifts the equilibrium to the side with the fewer moles of gas (i.e. for methanation, steam-methane reforming and oxidation reactions) [57–59]. For the decomposition reactor, the simulation modeled the fuel as a simple

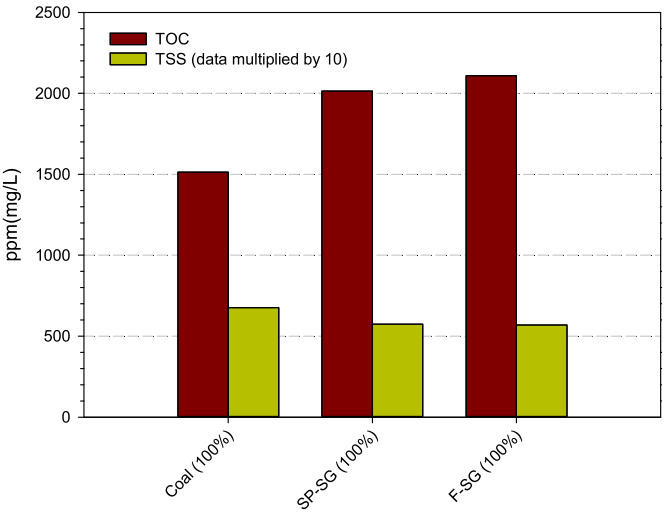

Fig. 14. Condensed water TOC and TSS for steam gasification of 100% coal, 100% SP-SG and 100% F-SG in atmospheric bubbling fluidized bed. Temperatures are given in Fig. 13.

Please cite this article in press as: Masnadi MS, et al., Single-fuel steam gasification of switchgrass and coal in a bubbling fluidized bed: A comprehensive parametric reference for co-gasification study, Energy (2014), http://dx.doi.org/10.1016/j.energy.2014.11.054

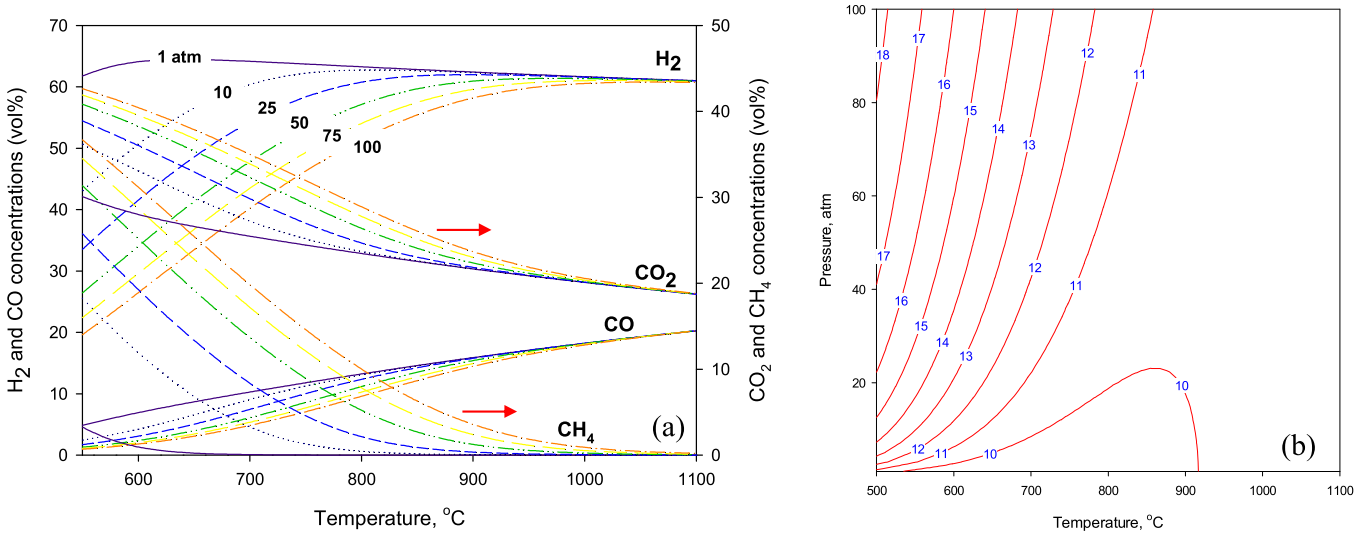

Fig. 15. Effect of temperature and pressure (1–100 atm) on (a) H_2, CO, CH_4 and CO_2 equilibrium compositions (b) HHV contours for 100% F-SG steam gasification with SF = 2.41.

combination of elements based on the ultimate analysis. Therefore, the model did not predict tar, char and heavier hydrocarbon elements. It also significantly under-estimated the methane concentration, reflecting the relative stability of CH_4, retarding its breakdown into equilibrium products [54,65].

The higher heating value of the product gas, calculated based on Equation (4) is predicted to increase as a result of decreasing the temperature and increasing the pressure, due to enhanced methane production, as shown in Fig. 15(b).

The effects of temperature and pressure on SO_2, H_2S, COS, NH_3, HCN, C_2H_2, C_2H_4, C_2H_6 and C_3H_8 equilibrium compositions for 100% F-SG steam gasification are shown in Fig. 16. The most concentrated side-product is H_2S, whose concentration increased as a result of lowering the temperature and raising the pressure. Sulfur

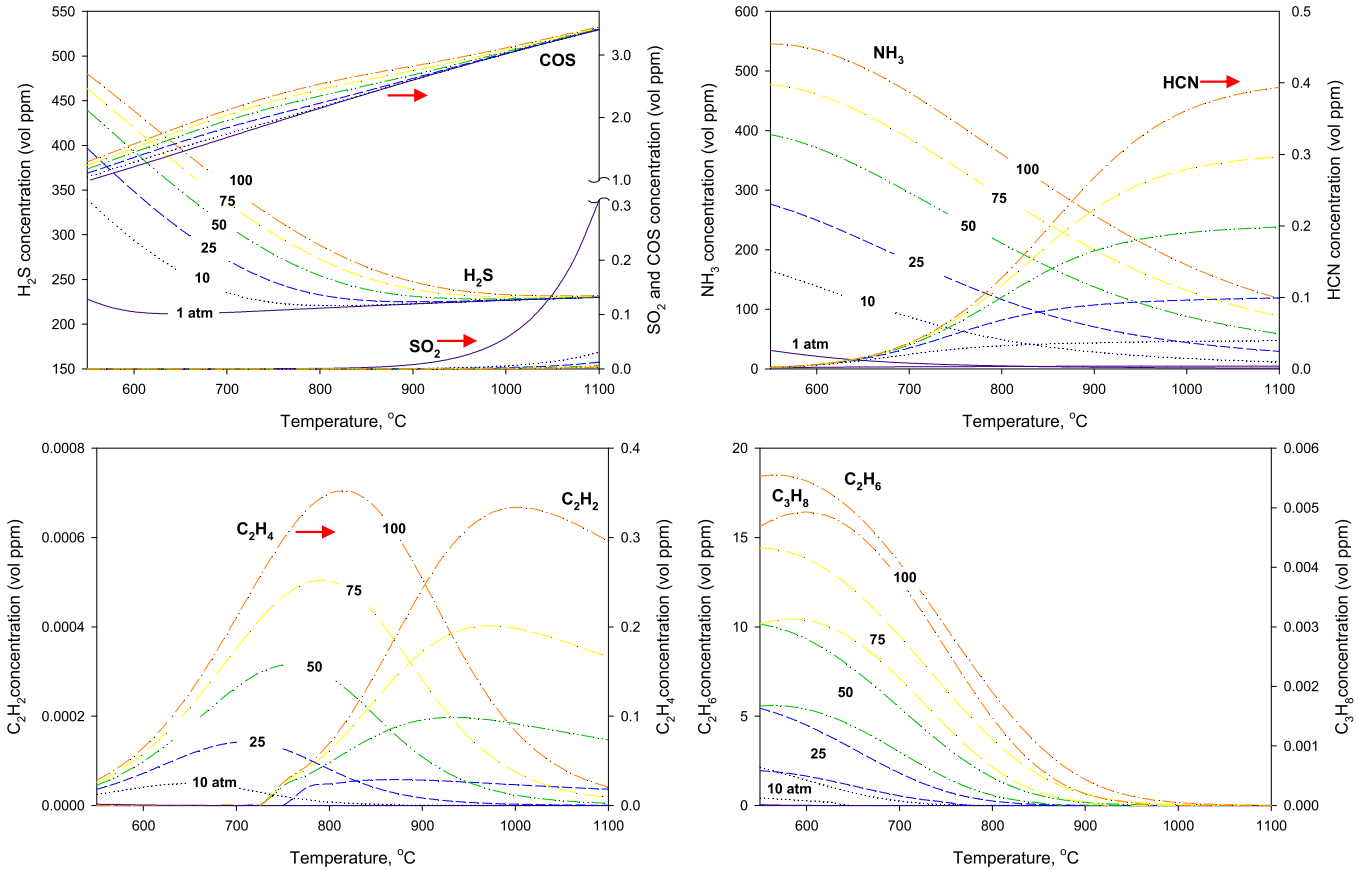

Fig. 16. Effect of temperature and pressure on SO_2, H_2S, COS, NH_3, HCN, C_2H_2, C_2H_4, C_2H_6 and C_3H_8 equilibrium compositions for 100% F-SG steam gasification with SF = 2.41.

Please cite this article in press as: Masnadi MS, et al., Single-fuel steam gasification of switchgrass and coal in a bubbling fluidized bed: A comprehensive parametric reference for co-gasification study, Energy (2014), http://dx.doi.org/10.1016/j.energy.2014.11.054

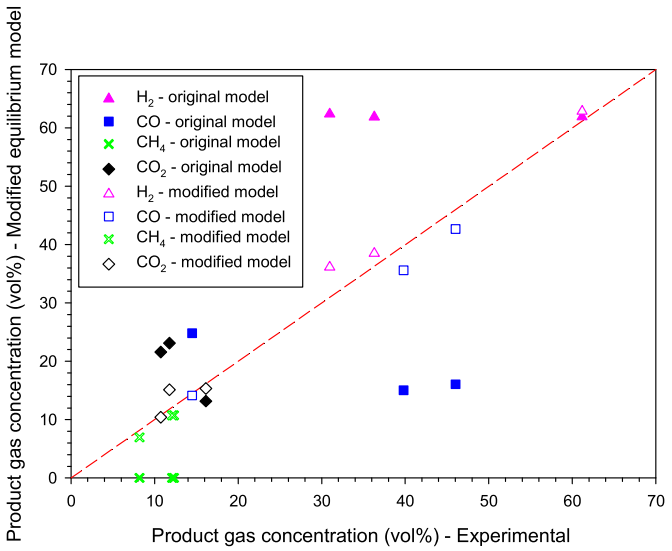

Fig. 17. Parity plot comparing experimental data with original and kinetically modified equilibrium model product gas compositions for 100% coal, SP-SG and F-SG steam gasification experiments at ~860 °C, SF ≈ 2.4 and 1 atm.

compounds corrode metallic surfaces [60]. Even small amount of sulfur can poison gasification catalysts [61]. Sulfur removal to parts per billion levels is often required in order to avoid these kinds of detrimental effects [46]. The molar fractions of HCN and NH_3 are sufficient to trace the two most important reaction pathways for nitrogen chemistry in combustion and gasification. These two species are important final products under reducing conditions, as well as key intermediate species for NO and N_2O formation in oxidizing atmospheres [62,63]. Although most of the ammonia decomposes to N_2 at typical gasification temperatures, its concentration should be controlled. Gas turbines usually demand ammonia concentrations less than 0.05 mL L^{-1} to control nitrogen oxide emissions, while less than 0.05 mL L^{-1} may still poison some catalysts used to upgrade syngas [64]. Acid gas removal units used for sulfur recovery can also experience problems unless nitrogen is substantially reduced [46,60]. Our results are in favorable agreement with equilibrium data reported by Li et al. [65].

3.2.2. Comparison of model predictions with experimental results

As shown in Fig. 17, for coal steam gasification, the "original" equilibrium model was able to predict with reasonable accuracy the H_2 and CO_2 concentrations (~61 vol% and 16 vol%, respectively). However, CO is over-predicted, presumably because the Boudouard reaction did not reach equilibrium. The model, on the other hand, fits poorly for biomass gasification due to model limitations, e.g. not considering the pyrolysis of the biomass with high volatile content (rich in CO [45]) or selective catalytic effects of switchgrass potassium on the Boudouard and steam-carbon gasification reactions.

Previous studies [66,67] have shown that high measured concentrations of methane from coal gasification result from incomplete conversion of pyrolysis products; equilibrium molar concentrations of methane in the off-gas are less than 0.1% for all runs, whereas actual methane concentrations are of the order of a few per cent. The high measured methane concentration in the product gas cannot be explained on an equilibrium or thermodynamic basis. The deviation must result from non-equilibrium factors, e.g. incomplete cracking of pyrolysis products. It is often taken for granted that the amount of each element participating in the chemical equilibrium is the same as for the feed. This is true when slow reaction kinetics and mass transfer processes do not impede the achievement of equilibrium. However, this assumption is not valid for real processes in which reactions (mostly heterogeneous) are influenced by kinetics and/or mass transfer limitations so that some elements and species never achieve equilibrium [65]. The model assumes that all reactions proceed to equilibrium, in which case the methane would mostly be reformed into H_2, CO and CO_2 at elevated temperatures and excess H_2O. With the addition of forced production of CH_4 and C_2+, in particular ethylene, a better fit could be obtained, as suggested by Li et al. [65] whose model included bypass for a portion of the fuel C and H to form CH_4.

For a steam-to-coal mass ratio range of 1–4, the original equilibrium modeling product gas composition and HHV data followed the same trend as the experimental results, see Fig. 18. Increasing steam shifted the equilibrium of product gas towards H_2 and CO_2, whereas CO and CH_4 decreased. Again the calculated HHV of the product gas declined, mainly because of the drop in CH_4 and CO. The model gave more accurate predictions at higher SF. Coal particles with high fixed carbon were not reactive enough for increasing steam-to-coal ratio to move the gasification reactions further towards equilibrium.

3.2.2.1. Modified equilibrium modeling results. As shown above, the high measured methane concentration in the product gas cannot be explained on an equilibrium or thermodynamic basis. The carbon conversion in a real gasifier depends on many factors: thermodynamics, chemical kinetics, hydrodynamics, heat and mass transfer, residence time and particle size distribution. Equilibrium

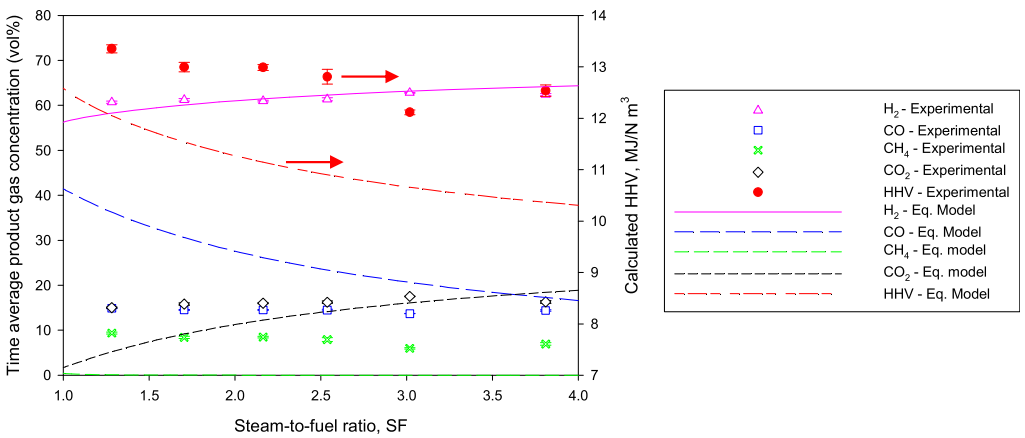

Fig. 18. Comparison of experimental data and equilibrium modeling predictions: effect of steam-to-fuel mass ratio on dry gas composition and HHV for 100% coal run.

Please cite this article in press as: Masnadi MS, et al., Single-fuel steam gasification of switchgrass and coal in a bubbling fluidized bed: A comprehensive parametric reference for co-gasification study, Energy (2014), http://dx.doi.org/10.1016/j.energy.2014.11.054

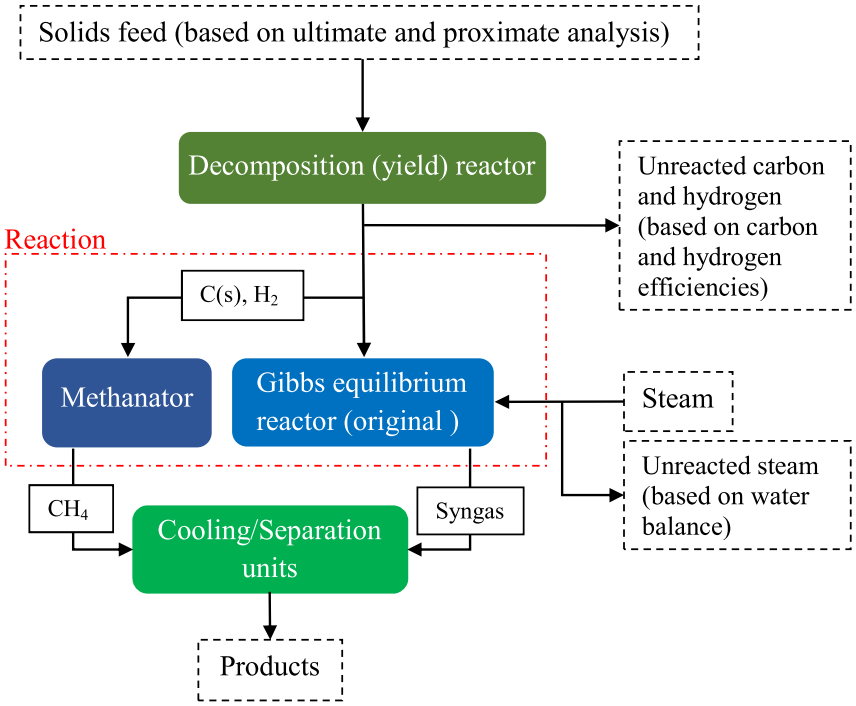

Fig. 19. Schematic of kinetically modified equilibrium model for steam gasification process.

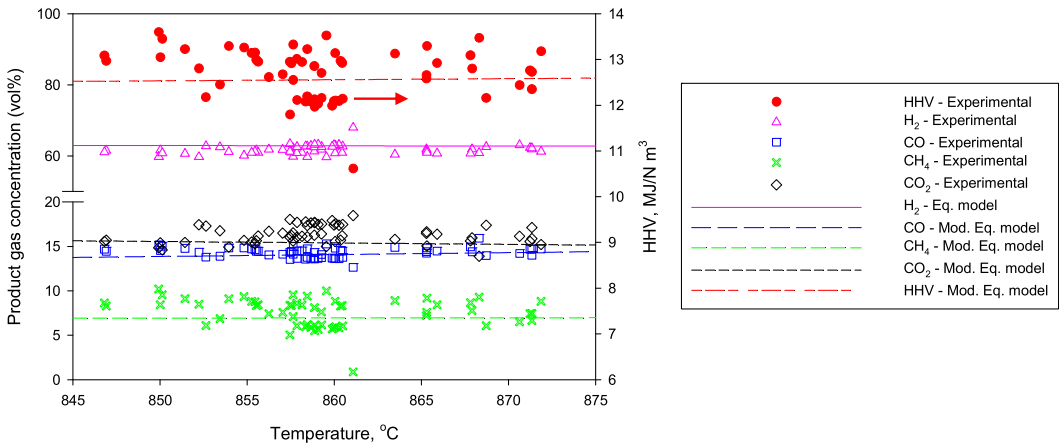

Fig. 20. Comparison of experimental data and modified equilibrium modeling predictions: effect of temperature on dry gas composition and HHV for 100% coal.

conversion provides an upper bound on the conversion efficiency, while the fractional achievement of equilibrium for a real system depends on such operating parameters as temperature, system pressure and steam-to-carbon ratio [65].

The discrepancy between the equilibrium model and experimental data can be substantially reduced if experimental data, such as the overall carbon, hydrogen and steam conversions, and the produced methane molar concentration, are used to modify the equilibrium model. As illustrated in Fig. 19, based on the experimental CH_4 molar data, a fraction of carbon and hydrogen was split from the decomposition reactor output stream and sent to a methanator stoichiometric reactor. The CH_4 produced according to reaction (14) was then combined with the Gibbs reactor products downstream. In addition, fractions of the C(s), H_2 and H_2O were removed from the decomposed feed and steam streams, based on the experimental carbon, hydrogen and water conversion efficiencies. See Ref. [12] for more details. From the parity plot in Fig. 17, it is evident that the modeling product gas composition predictions were enhanced significantly due to kinetic modifications based on the experimental data. We also find good agreement between the empirical and modified model data of the 100% coal steam gasification, as portrayed in Fig. 20.

4. Conclusions

As a basis for investigating biomass/fossil fuel co-gasification and to demonstrate the key characteristics of biomass and coal thermochemical conversion, single fuels (coal, spring switchgrass and fall switchgrass) were steam gasified in a pilot scale bubbling fluidized bed reactor at ~860 °C and 1 atm. Here are the main conclusions:

1) Steam gasification of Vancouver Island coal resulted in higher H_2/CO molar ratio and CO_2 concentration and lower CH_4

Please cite this article in press as: Masnadi MS, et al., Single-fuel steam gasification of switchgrass and coal in a bubbling fluidized bed: A comprehensive parametric reference for co-gasification study, Energy (2014), http://dx.doi.org/10.1016/j.energy.2014.11.054

production than for gasification of spring and fall switchgrass samples, due to the higher carbon content of the coal and therefore more steam-carbon reactions.

2) Steam gasification of biomasses rich in potassium resulted in H_2/CO molar ratios <1, presumably due to dominance of the Boudouard and steam-carbon endothermic reactions. Switchgrass potassium can catalyze these two reactions. Switchgrass contains more cellulose than coal and cellulose is known to convert to CO during the pyrolysis stage.
3) F-SG gasification resulted in higher carbon, hydrogen and cold gas efficiencies than for SP-SG gasification, possibly due to higher potassium concentration and hence, greater reactivity of the F-SG.
4) The equilibrium calculations showed that the steam-carbon reaction was in equilibrium for the experiments. The syngas sampling port location is important for this analysis.
5) An equilibrium model was programmed in Aspen Plus, based on minimization of steam gasification Gibbs free energy. The original model which excluded tar, char and heavy hydrocarbons was unable to predict the methane composition properly due to the simplifying assumptions. The modeling predictions were in better accord with the 100% coal experimental data than with biomass experimental data, in particular over-predicting the hydrogen concentration. This might be due to higher volatile content of switchgrass than coal. The original equilibrium model was kinetically modified by empirical data to account for the deviation from experimental results due to partial carbon and steam conversion. The modified model predictions compared reasonably well with measured gas compositions for the single-fuel experiments.

Acknowledgment

The authors gratefully acknowledge financial support from the Natural Sciences and Engineering Research Council (NSERC).

Appendix A. Supplementary data

Supplementary data related to this article can be found at http://dx.doi.org/10.1016/j.energy.2014.11.054.

References

[1] NOAA National climate data center. Selected significant climate anomalies and events. 2012–2014. published online, retrieved July 9, 2014 from, http://www.ncdc.noaa.gov/sotc/global/2014/1.
[2] United Nations Intergovernmental Panel on Climate Change. Climate change 2013: the physical science basis. Working Group I Contribution to the IPCC Fifth Assessment Report (AR5). New York: Cambridge Univ Press; 2013.
[3] United Nations Intergovernmental Panel on Climate Change. Climate change 2014: impacts, adaptation, and vulnerability. Working Group II Contribution to the IPCC Fifth Assessment Report (AR5). New York: Cambridge Univ Press; 2014.
[4] United Nations Intergovernmental Panel on Climate Change. Climate change 2014: mitigation of the climate change. Working Group III Contribution to the IPCC Fifth Assessment Report (AR5). New York: Cambridge Univ Press; 2014.
[5] Environment Canada. National inventory report 1990–2011: greenhouse gas sources and sinks in Canada. 2013.
[6] OECD/IEA. IEA key world energy statistics. 2013. Paris, France.
[7] Spath PL, Dayton DC. Preliminary screening-technical and economic assessment of synthesis gas to fuels and chemicals with emphasis on the potential for biomass-derived syngas. No. NREL/TP-510-34929, National Renewable Energy Lab Golden Co. 2003.
[8] U.S. Energy Information Administration (EIA). Annual energy outlook 2013 with projections to 2040. Washington, DC, USA: EIA; 2013.
[9] International Energy Agency (IEA). 21st Century coal advanced technology and global energy solution. Paris, France: IEA Coal Industry Advisory Board (CIAB); 2013.
[10] McLaughlin SB, Bouton J, Bransby D, Conger BV, Ocumpaugh WR, Parrish DJ, et al. Developing switchgrass as a bioenergy crop. In: Janick J, editor. Perspectives on new crops and new uses. Alexandria, VA: ASHS Press; 1999. p. 282–99.
[11] Keshwani DR, Cheng JJ. Switchgrass for bioethanol and other value-added applications: a review. Bioresour Technol 2009;100(4):1515–23.
[12] Masnadi MS. Biomass/fossil fuel co-gasification with and without integrated CO_2 capture. Ph.D. thesis. University of British Columbia; 2014.
[13] Masnadi MS, Grace JR, Bi XT, Lim CJ, Ellis N, Li YH, et al. From coal towards renewables: catalytic/Synergistic effects during steam co-gasification of switchgrass and coal in a pilot-scale bubbling fluidized bed reactor. [under review].
[14] Madakadze IC, Samson DL, Smith DL, Coulman BE. The phonological development and yield of warm season grasses in SW Quebec. Can J Plant Sci 1996;76:354.
[15] Parrish DJ, Wolf DD, Daniels WL, Vaughn DH, Cundiff JS. Perennial species for optimum production of herbaceous biomass in the Piedmont. Oak Ridge National Lab., TN (USA); Virginia Polytechnic Inst. and State Univ., Blacksburg, VA, USA; 1990.
[16] Sanderson MA, Reed RL, McLaughlin SB, Wullschleger SD, Conger BV, Parrish DJ, et al. Switchgrass as a sustainable bioenergy crop. Bioresour Technol 1996;56(1):83–93.
[17] Masnadi MS, Grace JR, Bi XT, Lim CJ, Ellis N. From fossil fuels towards renewable: inhibitory and catalytic effects of carbon thermochemical conversion during co-gasification of biomass and fossil fuels. Appl Energy 2015 [in press].
[18] Habibi R, Kopyscinski J, Masnadi MS, Lam J, Grace JR, Mims CA, et al. Co-gasification of biomass and non-biomass feedstocks: synergistic and inhibition effects of switchgrass mixed with sub-bituminous coal and fluid coke during CO_2 gasification. Energy & Fuels 2012;27(1):494–500.
[19] Pullen JR. Catalytic coal gasification. London: IEA Coal Research; 1984.
[20] Masnadi MS, Habibi R, Kopyscinski J, Hill JM, Bi X, Lim CJ, et al. Fuel characterization and co-pyrolysis kinetics of biomass and fossil fuels. Fuel 2013;117(Part B):1204–14.
[21] Delgado J, Aznar MP, Corella J. Calcined dolomite, magnesite, and calcite for cleaning hot gas from a fluidized bed biomass gasifier with steam: life and usefulness. Ind Eng Chem Res 1996;35(10):3637–43.
[22] Pfeifer C, Koppatz S, Hofbauer H. Steam gasification of various feedstocks at a dual fluidised bed gasifier: impacts of operation conditions and bed materials. Biomass Convers Biorefinery 2011;1(1):39–53.
[23] Watkinson AP, Li Y, Haligva J. High grade synfuels –phase 1. 2010. IRAP Project 709261.
[24] Sjöström K, Chen G, Yu Q, Brage C, Rosén C. Promoted reactivity of char in co-gasification of biomass and coal: synergies in the thermochemical process. Fuel 1999;78(10):1189–94.
[25] Haider A, Levenspiel O. Drag coefficient and terminal velocity of spherical and nonspherical particles. Powder Technol 1989;58(1):63–70.
[26] Grace JR. Fluidized bed hydrodynamics. In: Hetsroni G, editor. Handbook of Multiph. Syst.; 1982.
[27] D.D. CEN. TS 15439 biomass gasification—tar and particles in product gases sampling and analysis. 2006. CEN Tech. Specif.
[28] Andrew D. Method # 2540. Standard methods for the examination of water and wastewater. 5th ed. , Washington, DC: American Public Health Association; 2005. p. 2–56.
[29] Lide DR. CRC handbook of chemistry and physics 2004-2005: a ready-reference book of chemical and physical data. CRC press; 2004.
[30] Lv PM, Xiong ZH, Chang J, Wu CZ, Chen Y, Zhu JX. An experimental study on biomass air-steam gasification in a fluidized bed. Bioresour Technol 2004;95(1):95–101.
[31] Herguido J, Corella J, Gonzalez-Saiz J. Steam gasification of lignocellulosic residues in a fluidized bed at a small pilot scale. Effect of the type of feedstock. Ind Eng Chem Res 1992;31(5):1274–82.
[32] Turn S, Kinoshita C, Zhang Z, Ishimura D, Zhou J. An experimental investigation of hydrogen production from biomass gasification. Int J Hydrogen Energy 1998;23(8):641–8.
[33] James AK, Helle SS, Thring RW, Rutherford PM, Masnadi MS. Investigation of air and air-steam gasification of high carbon wood ash in a fluidized bed reactor. Energy Environ Res 2014;4(1). p. 15.
[34] Antal MJ. The effects of residence time, temperature and pressure on the steam gasification of biomass. Biomass as a nonfossil fuel source. ACS Publications; 1981. p. 313–34.
[35] Antal Jr MJ, Edwards WH, Friedman HL, Rogers FE. Study of the steam gasification of organic wastes. Princeton Univ., NJ (USA). Dept. of Mechanical and Aerospace Engineering; 1984.
[36] Kumar A, Jones DD, Hanna MA. Thermochemical biomass gasification: a review of the current status of the technology. Energies 2009;2(3):556–81.
[37] Kumar A, Eskridge K, Jones DD, Hanna MA. Steam–air fluidized bed gasification of distillers grains: effects of steam to biomass ratio, equivalence ratio and gasification temperature. Bioresour Technol 2009;100(6):2062–8.
[38] Gupta AK, Cichonski W. Ultra-high temperature steam gasification of biomass and solid wastes. Environ Eng Sci 2007;24(8):1179–89.
[39] Lucas C, Szewczyk D, Blasiak W, Mochida S. High-temperature air and steam gasification of densified biofuels. Biomass Bioenergy 2004;27(6):563–75.
[40] González JF, Román S, Bragado D, Calderón M. Investigation on the reactions influencing biomass air and air/steam gasification for hydrogen production. Fuel Process Technol 2008;89(8):764–72.

[41] Xu Q, Pang S, Levi T. Reaction kinetics and producer gas compositions of steam gasification of coal and biomass blend chars, part 1: experimental investigation. Chem Eng Sci 2011;66(10):2141–8.
[42] Vlaev LT, Markovska IG, Lyubchev LA. Non-isothermal kinetics of pyrolysis of rice husk. Thermochim Acta 2003;406(1):1–7.
[43] Boateng AA, Walawender WP, Fan LT, Chee CS. Fluidized-bed steam gasification of rice hull. Bioresour Technol 1992;40(3):235–9.
[44] Maniatis K, Buekens A. Fluidized bed gasification of biomass. EPE Rev Energ Prim 1982;17(3–4):25–39.
[45] Yang H, Yan R, Chen H, Lee DH, Zheng C. Characteristics of hemicellulose, cellulose and lignin pyrolysis. Fuel 2007;86:1781–8.
[46] Woolcock PJ, Brown RC. A review of cleaning technologies for biomass-derived syngas. Biomass Bioenergy 2013;52:54–84.
[47] Bridgwater AV. The technical and economic-feasibility of biomass gasification for power generation. Fuel 1995;74(5):631–53.
[48] Hepola J, McCarty J, Krishnan G, Wong V. Elucidation of behavior of sulfur on nickel-based hot gas cleaning catalysts. Appl Catal B Environ 1999;20(3):191–203.
[49] Iwaki H, Ye S, Katagiri H, Kitagawa K. Wastepaper gasification with CO_2 or steam using catalysts of molten carbonates. Appl Catal A Gen 2004;270(1):237–43.
[50] Jin G, Iwaki H, Arai N, Kitagawa K. Study on the gasification of wastepaper/carbon dioxide catalyzed by molten carbonate salts. Energy 2005;30(7):1192–203.
[51] Mckee DW. Mechanisms of the alkali metal catalysed gasification of carbon. Fuel 1983;62(2):170–5.
[52] Adinberg R, Epstein M, Karni J. Solar gasification of biomass: a molten salt pyrolysis study. J Sol energy Eng 2004;126(3):850–7.
[53] Smith WR, Missen RW. Chemical reaction equilibrium analysis: theory and algorithms. Wiley New York; 1982.
[54] Li XT, Grace JR, Lim CJ, Watkinson AP, Chen HP, Kim JR. Biomass gasification in a circulating fluidized bed. Biomass Bioenergy 2004;26(2):171–93.
[55] Peng D-Y, Robinson DB. A new two-constant equation of state. Ind Eng Chem Fundam 1976;15(1):59–64.
[56] Zanzi R, Sjöström K, Björnbom E. Rapid pyrolysis of agricultural residues at high temperature. Biomass Bioenergy 2002;23(5):357–66.
[57] Higman C, Van der Burgt M. Gasification. Gulf professional publishing, Access Online via Elsevier; 2011.
[58] Sue-A-Quan TA, Watkinson AP, Gaikwad RP, Lim CJ, Ferris BR. Steam gasification in a pressurized spouted bed reactor. Fuel Process Technol 1991;27:67.
[59] Fermoso J, Arias B, Plaza MG, Pevida C, Rubiera F, Pis JJ, et al. High-pressure co-gasification of coal with biomass and petroleum coke. Fuel Process Technol 2009;90(7–8):926–32.
[60] Lovell R, Dylewski S, Peterson C. Control of sulfur emissions from oil shale retorts. Report No.: EPA 600/7-82-016, Cincinnati, Ohio. 1981. p. 190.
[61] Dou BL, Zhang MC, Gao JS, Shen WQ, Sha XZ. High temperature removal of NH_3, organic sulfur, HCl, and tar component from coal-derived gas. Ind Eng Chem Res 2002;41(17):4195–200.
[62] Miller JA, Bowman CT. Mechanism and modeling of nitrogen chemistry in combustion. Prog Energy Combust Sci 1989;15(4):287–338.
[63] Mann MD, Collings ME, Botros PE. Nitrous oxide emissions in fluidized-bed combustion: fundamental chemistry and combustion testing. Prog Energy Combust Sci 1992;18(5):447–61.
[64] Zhou J, Masutani SM, Ishimura DM, Turn SQ, Kinoshita CM. Release of fuel-bound nitrogen in biomass during high temperature pyrolysis and gasification. In: 32nd Intersociety Energy Conversion Engineering Conference, July 22–August 1; 1997. p. 1785–90.
[65] Li X, Grace JR, Watkinson AP, Lim CJ, Ergüdenler A. Equilibrium modeling of gasification: a free energy minimization approach and its application to a circulating fluidized bed coal gasifier. Fuel 2001;80(2):195–207.
[66] Von Fredersdorff CG, Elliott MA. Coal gasification. Chem Coal Util 1963.
[67] Coates RL, Chen CL, Pope BJ. Coal devolatilization in a low pressure, low residence time entrained flow reactor. Coal Gasif 1974:92–8.
[68] Masnadi MS, Grace JR, Bi XT, Ellis N, Lim CJ, Butler JW. From fossil fuels towards more sustainable energy systems: biomass/coal steam co-gasification integrated with in-situ CO_2 capture. [under review].
[69] Yu MM, Masnadi MS, Grace JR, Bi X, Lim CJ, Li Y. Co-gasification of biosolids with biomass: thermogravimetric analysis and pilot scale study in a bubbling fluidized bed reactor. Bioresour Technol 2015;175:51–8.

Please cite this article in press as: Masnadi MS, et al., Single-fuel steam gasification of switchgrass and coal in a bubbling fluidized bed: A comprehensive parametric reference for co-gasification study, Energy (2014), http://dx.doi.org/10.1016/j.energy.2014.11.054